Spiral Crystal Growth in Blends of Poly(vinylidene fluoride) and Poly(vinyl acetate)

Yoshifumi Okabe,[†] Thein Kyu,*[,†] Hiromu Saito,[‡] and Takashi Inoue[‡]

Institute of Polymer Engineering, The University of Akron, Akron, Ohio 44325, and Department of Organic and Polymeric Materials, Tokyo Institute of Technology, Meguro-ku, Tokyo 152-8552, Japan

Received April 27, 1998; Revised Manuscript Received June 29, 1998

ABSTRACT: Crystallization behavior and morphology development in miscible blends of poly(vinylidene fluoride) (PVDF) and poly(vinyl acetate) (PVAc) have been investigated on the basis of light scattering, optical microscopy, and atomic force microscopy (AFM). Strikingly, a spiral crystal growth was observed at the core of the spherulites in the pure PVDF as well as in its blends with PVAc. The spiral structure appears to emerge from the aggregation of microfibrils during crystallization. The AFM study revealed that the microfibrils at the core are partially aligned with their long axes parallel to the spiral axis during the initial growth stage, but the fiber axes gradually change their orientation in the perpendicular direction as the spiral wave propagates toward an outer edge. The band periodicity was found to increase with increasing amorphous PVAc content. Furthermore, the periodic distance between neighboring spiral arms increases from the core to the outer edge, and this may be ascribed to the preferential rejection of PVAc chains into the inter-spiral regions during PVDF crystallization.

Introduction

Crystallization kinetics and subsequent morphology development in semicrystalline homopolymers have been studied exhaustively over a span of nearly a half-century.[1−17] One of the universally recognized features in the morphology of crystalline polymers is the development of spherulites.[6−9] Polymer spherulites refer to a hierarchy structure, featuring a spherical (often-truncated) shape in which aggregates of crystalline lamellae have grown from a common center in the radial direction. It is well-known that the nucleus of the spherulite is generally anisotropic, with microfibril aggregates forming bundles.[1−5] As crystallization proceeds, these microfibrils fan out, leading to a sheaflike or splay texture. These spherulites generally display a maltese cross extinction pattern under a polarized optical microscope due to the orientation of the crystal chains. Occasionally, the maltese crossed pattern is combined with the multiple concentric extinction rings. The spherulites composed of such extinction rings are termed "ringed or banded" spherulites.[3] These concentric extinction rings have been attributed to a periodic variation of birefringence in the radial direction associated with twisting of the lamellae. This lamellar twisting seems to be caused by a desperate attempt of the lamella to release the compressive stress arising from the opposing lamellar fold surfaces. A closer examination of the lamellar twist regions within the spherulites of semicrystalline polymers, e.g., polyethylene[1−9] and α-type poly(vinylidene fluoride)[10−12] revealed that the twisting is discontinuous, interleaving short and curved lamellae. The unequivocal assignment on the mechanism of the lamellar twisting, however, remains controversial, and thus it is subject to debate.

Despite numerous efforts to elucidate the crystallization habit and resulting morphology of polymers, there are several unsolved dilemmas. One of the unexplained phenomena, which has received little or no attention, is the spiral pattern at the center of the concentric extinction rings, found in some homopolymers.[7,9] The spirals are interpreted as a consequence of asymmetric fanning of sheaves, leading to the "twisting" on a dimension level that is beyond the twisting that is responsible for the concentric banding. However, the origin and dynamics of this spiral pattern have not been explained in terms of how the spiral pattern emerges at the core of the spherulite. A similar spiral growth pattern have been found to occur in some faceted single crystals at a much smaller length scale, e.g., with a spiral or a pyramid-type structure.[1] The origin of such spiral-type single crystals has been ascribed to a screw dislocation mechanism.[1−5]

In this paper, we focus our attention on the kinetic aspects of crystallization in miscible blends of poly(vinylidene fluoride) (PVDF) and poly(vinyl acetate) (PVAc).[18,19] We have investigated the crystallization behavior and morphology development of the PVDF/PVAc blends using light scattering, optical microscopy, and atomic force microscopy (AFM). Of particular interest is the observation of the spiral crystal growth of PVDF spherulites in the blends, succeeded by the growth of concentric ring patterns. The spiral spherulitic growth behavior has been examined as a function of composition and crystallization temperature.

Experimental Section

Poly(vinylidene fluoride) (PVDF) with a weight-average molecular weight (M_w) of 246 000 and a number-average molecular weight (M_n) of 144 000 was kindly supplied by Kureha Chemical Industry, Co., Ltd. Poly(vinyl acetate) (PVAc) was purchased from Scientific Polymer Products, Inc. Both polymers were dissolved together in the 1:1 ratio of *N*,*N*′-dimethyl acetamide (DMAc) and tetrahydrofuran (THF). The polymer concentration was 5 wt %. These polymer solutions were further mixed to the desired concentrations. The blend films were cast onto cover glasses via evaporation of the solvent at ambient temperature. The cast films were further dried under vacuum for 1 week at room temperature. The film specimens thus prepared were about 10 μm thick.

* To whom correspondence should be addressed.
[†] The University of Akron.
[‡] Tokyo Institute of Technology.

S0024-9297(98)00668-8 CCC: $15.00
Published on Web 08/06/1998

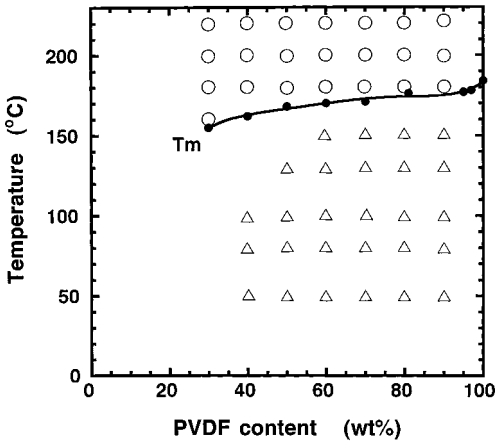

Figure 1. Phase diagram of PVDF/PVAc blends. The pseudoequilibrium melting temperature was estimated by extrapolating the light scattering data measured at 1.0 and 0.5 °C/min to zero heating rate. Key: (○) isotropic melt; (△) crystals.

To ensure complete removal of the solvent, the film specimens were melted at 200 °C in a hot stage for 10 min. These molten specimens were rapidly transferred to an optical microscope hot stage controlled at various experimental temperatures. The polarizing optical microscope used in this study was a Nikon Optiphot 2-pol equipped with a Nikon camera (FX-35DX) and a color-digital CCD (charge-coupled detector) camera (SSC-DC34, Sony) for image analysis. A "melting point versus composition" phase diagram of the PVDF/PVAc blends was established using small angle light scattering (SALS). The SALS instrument was equipped with a randomly polarized He−Ne laser operated at a power of 2 mW, (Model LSL2R, Aerotech, Inc.), a photomultiplier (HC-220-1, Hamamatsu Co.), a goniometer (ART 306, Aerotech Inc.), and a programmable heating stage (Omega CN-2012). The temperature at which the scattered intensity diminished abruptly was regarded as a melting point. The heating rate was varied from 1.0 to 0.5 °C/min. For surface morphology characterization, an atomic force microscope (AFM, Seiko Instruments, SPI-3,600), equipped with a Si_3N_4-type cantilever, was utilized.

Results and Discussion

A "melting temperature versus composition" phase diagram of the PVDF/PVAc blends as determined by light scattering is depicted in Figure 1. The nonequilibrium melting temperatures (T_m) were determined at 1.0 and 0.5 °C/min, and then the data were extrapolated to zero heating rate. The extrapolated data at zero heating rate have been regarded as a pseudoequilibrium melting temperature. Upon addition of PVAc, the depression of the PVDF melting temperature occurs, which is expected for a miscible pair containing crystalline constituents.[17−19] Upon heating above the T_m, the mixture remains homogeneous and transparent without any indication of phase separation, suggesting that the blend is completely miscible up to the maximum temperature investigated (230 °C). However, various spherulitic crystalline structures developed at temperatures below the T_m during cooling (shown by the triangles).

Isothermal crystallization studies were undertaken for the neat PVDF and its blends with PVAc as a function of composition and temperature. Parts a and b of Figure 2 depict the evolution of PVDF spherulites in the neat PVDF following a T quench from the melt (200 °C) to the isothermal crystallization temperature (T_c) of 165 °C. The core of the spherulite shows a single arm spiral pattern, rotating in the clockwise direction (Figure 2a). It should be emphasized that the spiral

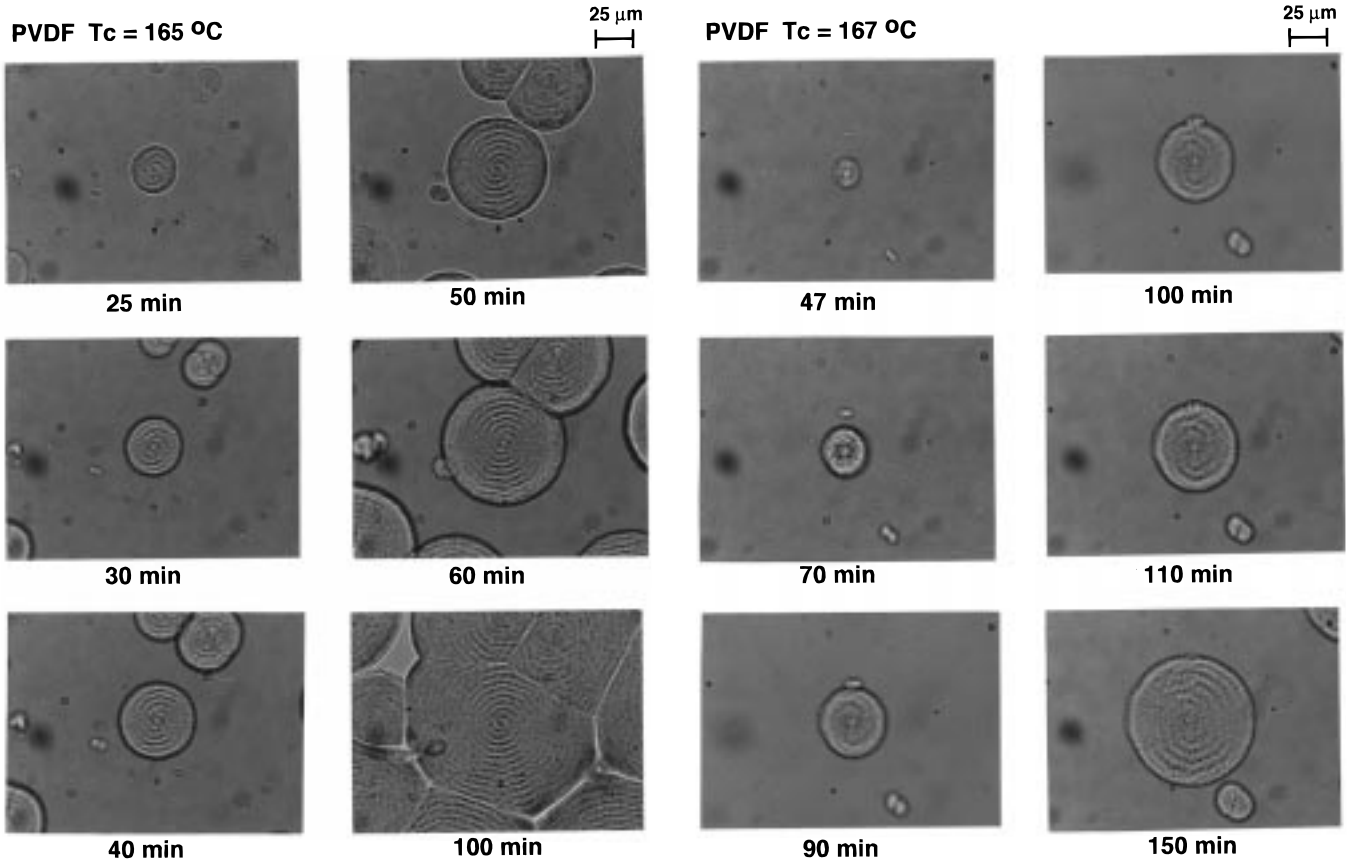

Figure 2. Time evolution of the spherulitic structure of the neat PVDF at an isothermal crystallization temperature of (a) 165 °C and (b) 167 °C, displaying spiral crystal growth patterns.

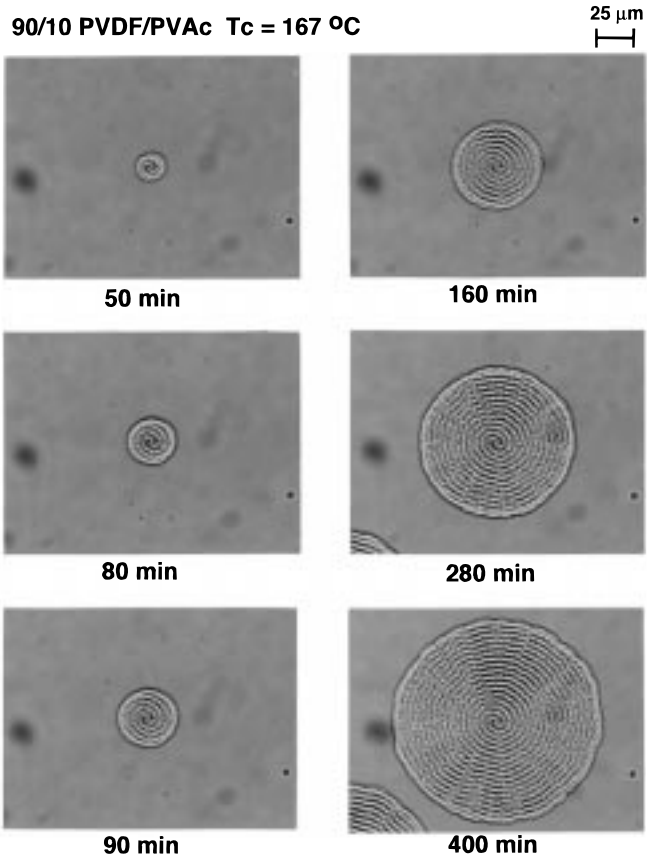

Figure 3. Time evolution of spherulitic patterns of the 90/10 PVDF/PVAc blends at various isothermal crystallization temperatures, displaying growth of a two-arm spiral in the counterclockwise direction at 167 °C.

growth could occur in both the clockwise and counterclockwise directions with equal probability. The average spherulitic size increases during crystallization until impingement occurs. A similar growth pattern has been observed at a T_c of 167 °C, except that the spiral pattern at the core of the spherulite is less distinct (Figure 2b). The onset time as well as the rate of crystallization at 167 °C have been retarded relative to that of 165 °C due to a smaller supercooling ($\Delta T = T_m - T_c$).[19]

Figure 3 depicts the evolution of the spherulitic structure in the 90/10 PVDF/PVAc blend at $T_c = 167$ °C, which is slightly below the pseudoequilibrium melting temperature. It required about 50 min to first discern the lamellar fragments (or fibrils) at the nuclei, which become more distinct after 80 min. These fibrils evolve into a spiral pattern that grows in time in the counterclockwise direction. It is striking to notice that the spiral pattern is a two-arm type, rotating in the same direction. The tips of the growing front are clearly identifiable during the initial periods (about 50, 80, and 90 min). Concurrently, the radius of the spherulite increases while the spiral tips grow along the periphery of the spherulite in the counterclockwise direction. At 280 min, the spiral growth ceases due to the collision with the inner spirals. However, the spherulite continues to grow, showing multiple concentric rings.

Similar growth behavior has been seen at $T_c = 170$ °C (Figure 4a), but the growth process has slowed significantly. It is apparent that the band periodicity is larger as compared to that at $T_c = 167$ °C. When the isothermal crystallization experiment was undertaken at a lower temperature of 165 °C, a similar spiral growth

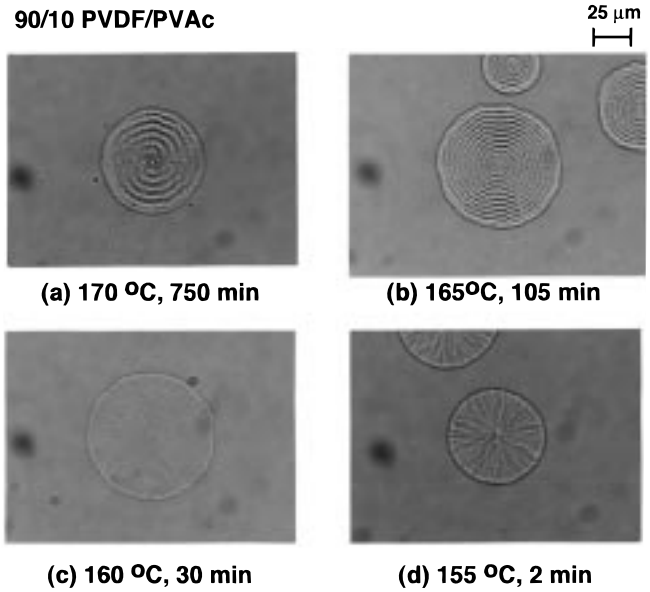

Figure 4. Emergence of PVDF spherulitic morphology in the 90/10 PVDF/PVAc blends, displaying (a) and (b) spiral, (c) concentric, and (d) lamellar splay textures with decreasing crystallization temperature in conjunction with the dependence of band periodicity on crystallization temperature.

pattern was discerned, except that the growth process is expedited (25 min) due to a larger supercooling (Figure 4b). Although the spherulitic growth front is nearly circular in the early stage of growth, the spherulitic boundary becomes wavy at the late stage of spherulitic growth before impingement. The isothermal crystallization at $T_c = 160$ °C shows the development of a much smaller band spacing (Figure 4c). The core of the spherulites appears to be a ring pattern. However, often the spiral and the concentric ring patterns are indistinguishable from each other. In some cases, both spiral and concentric ring patterns are found to coexist in the same sample, but at different locations. When isothermal crystallization was carried out at 155 °C, the spherulitic growth occurs in the form of the lamellar splay (radial growth) morphology in which the lamellae orient with their long axes in the radial direction by splaying outward from a common center (Figure 4d). It is therefore reasonable to infer that decreasing the isothermal crystallization temperature (i.e., increasing the supercooling) has resulted not only in a reduction of the band periodicity but also in the emergence of a variety of spherulitic structures such as spirals, concentric rings, and lamellar splay morphologies.

The observed change of the spherulite textures with temperature can further be confirmed in the 80/20 PVDF/PVAc composition. Figure 5 shows the emerging spherulite textures exhibiting the spiral, concentric ring, and lamellar splay morphologies in order of descending crystallization temperature. Note that the indicated times for the spherulite structures represent approximate elapsed times for the spherulites to reach a comparable size. The ultimate time required to reach the asymptotic limit decreases at lower crystallization temperatures. The band periodicity of the spiral or of the concentric ring decreases with decreasing crystallization temperature in both the 90/10 and 80/20 PVDF/PVAc blends (Figure 6).

When $T_c = 167$ °C, interesting spiral crystal growth behavior was observed in the 70/30 PVDF/PVAc blend (Figure 7). At around 190 min, two nuclei (circular

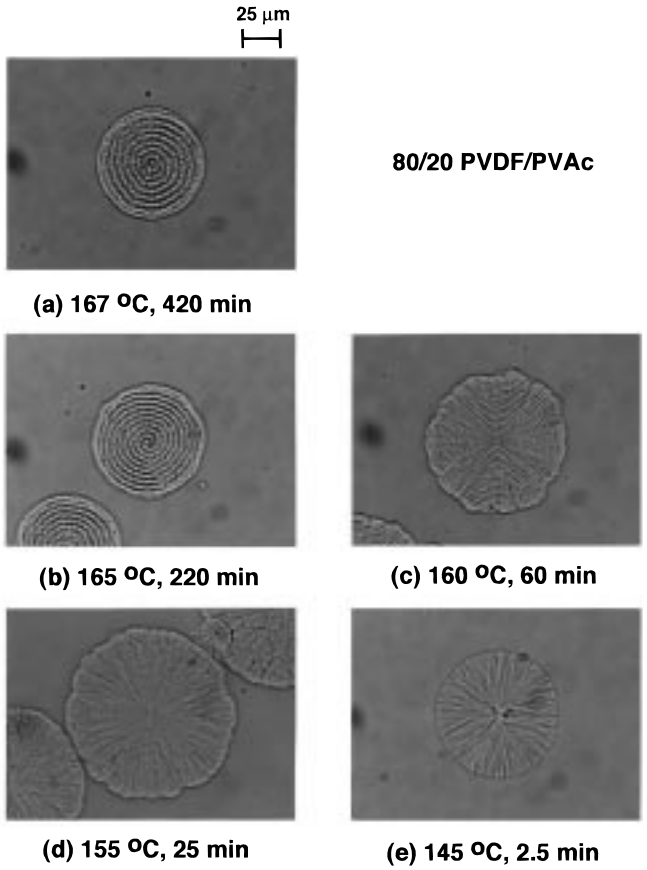

Figure 5. PVDF spherulites in the 80/20 PVDF/PVAc blends, displaying various textures during isothermal crystallization: (a) clockwise spiral at 167 °C, (b) counterclockwise at 165 °C, (c) wavy counterclockwise spiral at 160 °C, (d) concentric ring morphology at 155 °C, and (e) lamellar splay morphology at 145 °C. Indicated times represent the elapsed times required for the spherulites to reach a comparable size.

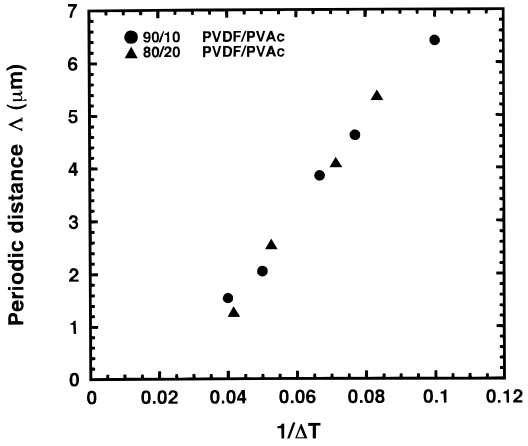

Figure 6. Dependence of the periodic distance on supercooling ΔT for the 90/10 and 80/20 PVDF/PVAc blends.

wave patterns) have seemingly collided and parts of the circular waves are fragmented. Subsequently, a two-arm spiral rotating in the clockwise direction is formed. The interesting point is that the original two-arm spiral becomes a four-arm spiral at 280 min. Subsequently, some of the arms cease to grow when they collide with the neighboring spirals. The four-arm spiral gradually transforms into a three-arm spiral (at 610 min) and then to a two-arm spiral (at 910 min). Another striking observation is that multiple arm spirals rotate in the clockwise direction in one spherulite (at the center of

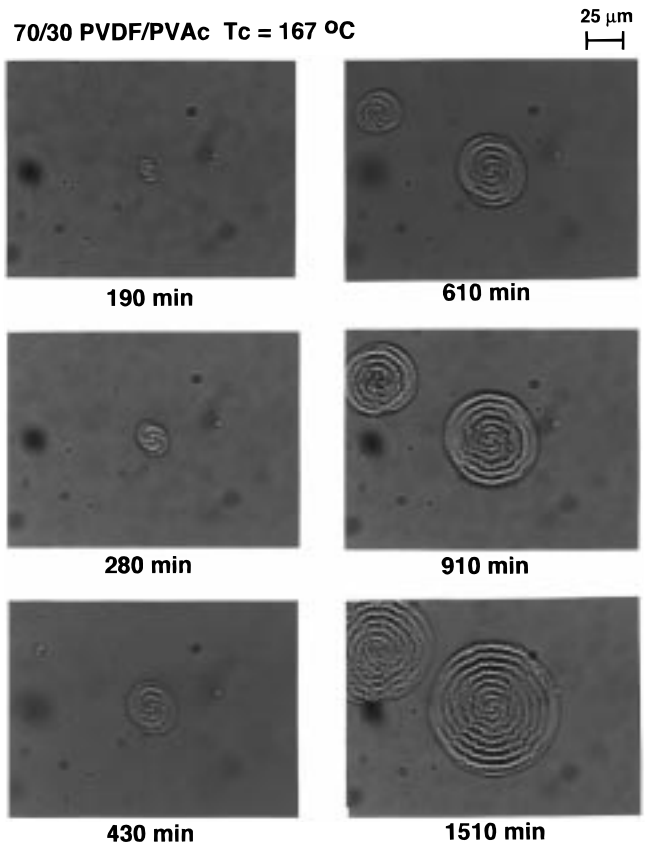

Figure 7. Time evolution of spherulitic patterns of the 70/30 PVDF/PVAc blends at an isothermal crystallization temperature of 167 °C, displaying the emergence of multiple arms into a two-arm spiral during crystallization.

Figure 7), but in the counterclockwise direction in the other (at the upper left corner of Figure 7).

The present study raises several intriguing questions: (i) why does crystal growth occur in a spiral wave pattern in the first place at high isothermal crystallization temperatures, (ii) what determines whether single-arm, or two-arm, or multiple-arm spirals form, and (iii) why are some spirals often twisted in opposite directions within the same specimen. The origin of this spiral crystal growth is not clearly understood at this time, but some definite features are noteworthy, as summarized in the morphology map (Figure 8). The spiral patterns are generally seen within the high crystallization temperature range across all compositions investigated. However, the concentric ring and lamellar splay morphologies develop at lower crystallization temperatures. Occasionally, the spiral and concentric ring patterns, denoted S/C in the phase diagram, are indistinguishable under an optical microscope due to the small band size at large supercooling. However, depolarized light scattering is capable of distinguishing the two structures because the higher angle scattering pattern characteristic of the ring structure is different from that of a spiral growth pattern. To probe the emergence of spiral/target patterns, a time-resolved depolarized light scattering study is still underway. The notation C/L implies that the concentric ring and lamellar splay morphology are either indistinguishable or overlapped. Although the blends of PVDF with ester-containing polymers have been studied exhaustively,[17−24] the present paper is probably the first to report the intricate morphology map for the PVDF/PVAC blend.

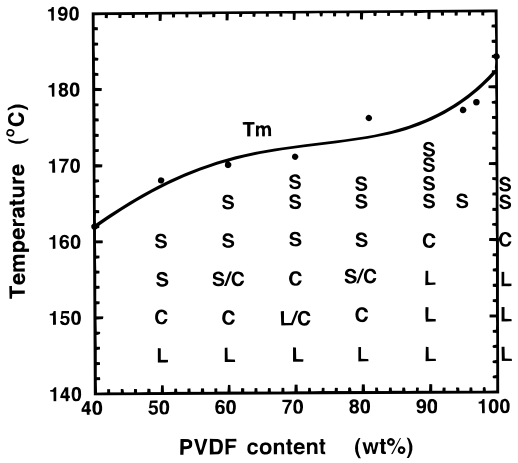

Figure 8. Morphology map of PVDF/PVAc blends at several isothermal crystallization temperatures and compositions: S, spiral; C, concentric rings; L, lamellar splay morphology.

It is well documented that PVDF crystallizes in the forms of α, γ, or γ' type crystals in the order of descending crystallization temperatures.[11,12,20] The α modification is known to occur predominantly as a stable form in the primary crystallization process below 150 °C. However, both the α and γ forms may occur when the crystallization temperature is in excess of 170 °C. The γ modification generally occurs as a secondary crystallization process through a crystal−crystal transformation. Occasionally, γ spherulites are embedded in preformed α-type spherulites.

In this paper, we focus on the spherulites. The α spherulites are commonly observed either in the form of concentric ring spherulites, of radial lamellar splay morphology, or of loosely packed spherulites (often called dendrites) having highly branched fibrils. However, the present spiral growth pattern is unique and has been largely overlooked in most studies of semicrystalline polymers and their blends. The reason for this is that most studies have been directed toward the crystallization behavior occurring at low crystallization temperatures where spiral and concentric ring spherulites are indistinguishable.

The spiral crystal growth at the core of the spherulite in the 90/10 PVDF/PVAc blend was further examined by AFM. The crystallization was carried out isothermally at 170 °C, in which the two-arm spiral was observed at the core of the spherulite, but the picture was taken on the quenched specimen at ambient temperature. The bright and dark spiral regions represent the depth profiles of the ridges and valleys, respectively (Figure 9). The ridges correspond to the bright region in the extinction spiral seen under the optical microscope. The microfibrils at the core were partially aligned with their long axes parallel to the spiral direction in the initial growth stage, but the fiber axes gradually become oriented in the perpendicular direction as the spiral wave propagates toward the outer ring. Thus, the mechanism of the spiral growth is different from that of the extinction rings such as concentric rings, which are generally thought to emerge from the molecular orientation of twisted lamellae. The microfibrils tend to self-assemble by aligning parallel with respect to each other, but along the direction perpendicular to the spiral growth. This process of self-organization of the microfibrils is reminiscent of layer ordering in smectic liquid crystals,[25] except that the

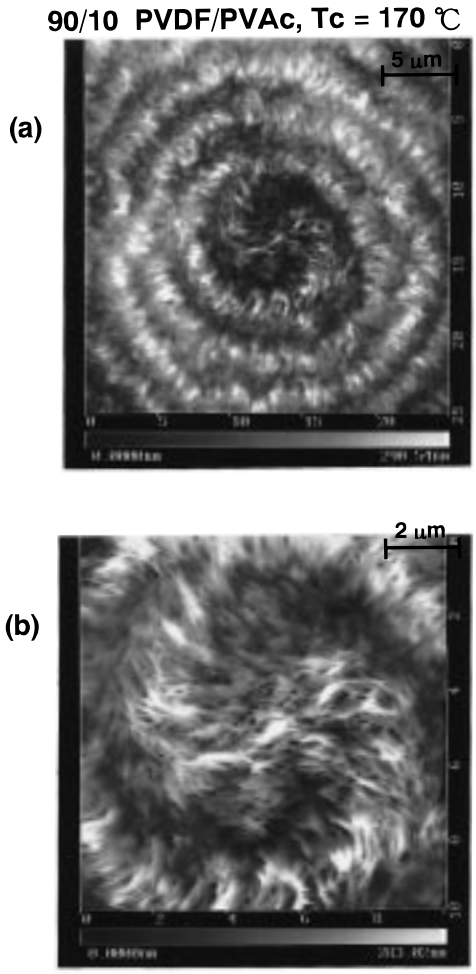

Figure 9. AFM picture of the 90/10 PVDF/PVAc blend at different magnifications, displaying spiral ridges and valleys consisting of self-assembled microfibrils. The blend specimen was crystallized at 170 °C, but the picture was obtained after quenching to room temperature.

length scale of the spirals (a few micrometers) is much larger than that of the smectic layers (in nanometer scale).

An interesting question is, what is the material composition in the inter-spiral region? One speculative answer is that the amorphous PVAc may be, along with some amorphous PVDF, rejected predominantly into these inter-spiral regions (valleys). Some microfibrils are seemingly present in these inter-spiral regions, but their concentration is small relative to those in the spiral ridges. The next question is, are those spiral ridges associated only with surface phenomena? If not, how are the spiral wave textures at the surface coupled with those in the bulk? Additional work is necessary to answer these fundamental questions, which is therefore left to the scope of a future study.[26]

Another interesting feature is that the band periodicity displays strong composition dependence. Figure 10 depicts the dependence of the length scale of the band periodicity on blend composition at an isothermal crystallization temperature of 160 °C. With increasing amorphous PVAc content, more amorphous materials have to be rejected from the crystallizing fronts into the inter-lamellar, inter-fibrillar, and inter-spiral regions. The lamellar long period is expected to increase if the amorphous PVAc chains were preferentially rejected into the inter-lamellar and inter-fibrillar regions. The

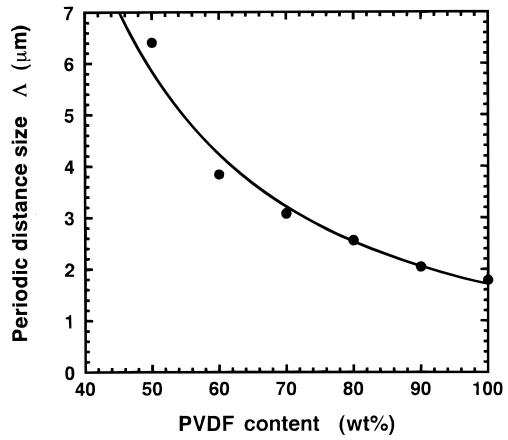

Figure 10. Distance between the second and third rings of the PVDF spherulite in the PVDF/PVAc blends as a function of PVDF content at an isothermal crystallization temperature of 160 °C.

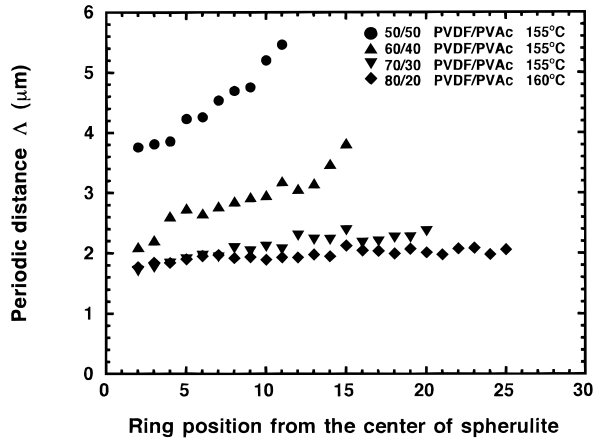

Figure 11. Periodic distances of the bands from the core to the outer rings of the PVDF spherulite for various blend compositions.

small-angle X-ray scattering and small angle light scattering studies are still in progress.[26] On the same token, the band periodicity should increase when amorphous PVAc are excluded into the inter-spiral regions (i.e., the valley between the spiral ridges) along with some amorphous PVDF chains. The latter scenario is supported by the fact that the band periodicity increases with increasing PVAc content (Figure 11).

The possible rejection of amorphous PVAc into the inter-spiral regions can be further confirmed in the isothermal crystallization by examining the band spacing from the core to the outer rings of the spherulite. Figure 11 shows the increasing periodic spacing during spiral growth; i.e., the distance between the neighboring spirals increases from the core to the outer edge, particularly in the PVAc rich blends (e.g., at 155 °C). This tendency disappears when the PVDF content is increased to 80%, despite the fact that the crystallization temperature was increased to 160 °C. Judging from the trend of the spiral spherulitic growth with increasing PVDF in Figure 11, it seems plausible that the crystallization in the pure PVDF may not show any dependence of the band size on the distance from the core. All the above observations point to the conclusion that the PVAc chains must therefore be rejected predominantly into the inter-spiral and inter-concentric ring regions. However, one cannot rule out the possibility that some amorphous PVDF chains could be rejected into the same inter-spiral regions due to their profound miscibility with PVAc chains. It is also likely that some amorphous PVAc chains would be rejected into inter-lamellar and inter-fibrillar regions.

Conclusions

The phenomenon of spiral crystal growth has been observed in the miscible PVDF/PVAc blends. The present paper is probably the first to systematically examine the spiral spherulitic growth in crystalline polymer blends, accompanied by growth of the concentric ring (target) structure. This spiral spherulitic growth occurs predominantly at high crystallization temperatures very close to the melting temperature. As expected, the band periodicity decreases with increasing supercooling. In descending order of crystallization temperature, the spherulite textures show spirals with single or multiple arms, concentric rings, and lamellar splay morphologies. The AFM study revealed that the microfibrils at the core are partially aligned with their long axes parallel to the spiral direction in the initial growth stage but gradually become oriented in the perpendicular direction as the spiral wave propagates toward the outer edge. It is likely that the amorphous PVAc chains would be rejected from the PVDF crystal fronts into the inter-lamellar, inter-fibrillar, and inter-spiral (inter-ring) regions of the growing spherulite. In this study, we are able to confirm the rejection of the amorphous PVAc chains into the inter-spiral and inter-ring regions using optical microscopy.

Acknowledgment. This work was supported in part by the National Science Foundation NSF Grant No. DMR 95-29296. The present collaboration would not have been possible without the Morton Distinguished Visiting Professorship (to T.I.) at the University of Akron. Y.O. thanks Sumitomo Electric Industries, Ltd., for their support of his study at the University of Akron.

References and Notes

(1) Geil, P. H. *Polymer Single Crystals*; Wiley-Interscience: New York, 1963.
(2) Wunderlich, B. *Macromolecular Physics*; Academic Press: New York, 1973 and 1976; vol. 1 and vol. 2.
(3) Basset, D. C. *Principles of Polymer Morphology*; Cambridge University Press: Cambridge, U.K., 1981.
(4) Khoury, F.; Passaglia, E. In *Treatise on Solid State Chemistry*; Hannay, N. B., Ed.; Crystalline and Noncrystalline Solids; Plenum Press: New York, 1976; Vol. 3.
(5) Barham, P. J. In *Materials Science and Technology*; Cahn, R. W., Hansen, P., Kramer, E. J., Eds.; Structure and Properties of Polymers; VCH Publishers: Weinheim, 1993; Vol. 12.
(6) Keller, A. *Nature* **1952**, *169*, 913.
(7) Keith, H. D.; Padden, F. J., Jr. *J. Polym. Sci.* **1959**, *39*, 101, 123.
(8) Price, F. P. *J. Polym. Sci.* **1959**, *39*, 139; **1961**, *54*, S40.
(9) Keller, A.; Warning, J. R. S. *J. Polym. Sci.* **1955**, *17*, 447. Keller, A. *J. Polym. Sci.* **1959**, *39*, 151.
(10) Singfield, K. L.; Hobbs, J. K.; Keller, A. *J. Cryst. Growth* **1998**, *183*, 683.
(11) Lovinger, A. J.; Keith, H. D. *Macromolecules* **1979**, *12*, 919.
(12) Lovinger, A. J. *J. Polym. Sci., Polym. Phys. Ed.* **1980**, *18*, 793.
(13) Keith, H. D.; Padden, F. J., Jr. *Polymer* **1984**, *25*, 28; *Macromolecules* **1996**, *29*, 7776.
(14) Vaughan, A. S. *J. Mater. Sci.* **1993**, *28*, 1805.
(15) Bassett, D. C.; Hodge, A. M. *Proc. R. Soc.* **1979**, *A359*, 121; *Polymer* **1978**, *19*, 469; *Proc. R. Soc.* **1981**, *A377*, 61.
(16) Keller, A.; Goldbeck-Wood, G. In *Comprehensive Polymer Science*, 2nd Supplement; Aggarwal, S. L., Russo, S., Eds.; Pergamon: Oxford, U.K., 1996; Chapter 7, p 241.
(17) Nishi, T.; Wang, T. T. *Macromolecules* **1975**, *8*, 909.

(18) Paul, D. R.; Barlow, J. W.; Bernstein, R. E.; Wahrmund, D. C. *Polym. Eng. Sci.* **1978**, *18*, 1225. Paul, D. R.; Barlow, J. W. *J. Macromol. Sci., Rev. Macromol. Chem.* **1980**, *C18*, 109.
(19) Olabisi, O.; Robeson, L. M.; Shaw, M. T. *Polymer−Polymer Miscibility*; Academic Press: New York, 1979.
(20) Morra, B. S.; Stein, R. S. *Polym. Eng. Sci.* **1984**, *5*, 311.
(21) Keith, H. D.; Padden, F. J., Jr.; Russell, T. P. *Macromolecules* **1989**, *22*, 666.
(22) Tomura, H.; Saito, H.; Inoue T. *Macromolecules* **1992**, *25*, 1611.
(23) Braun, D.; Jacobs, M.; Hellmann, G. P. *Polymer* **1994**, *35*, 706.
(24) Penning, J. P.; Manley, St. J. R. *Macromolecules* **1996**, *29*, 77, 84.
(25) Chandrasekhar, S. *Liquid Crystals*, 2nd Ed.; Cambridge University Press: Cambridge, U.K., 1992.
(26) Okabe, Y.; Saito, H.; Inoue, T.; Kyu, T. Manuscript in preparation.

MA980668M